Available online at www.sciencedirect.com
SCIENCE DIRECT®
European Journal of Cell Biology 84 (2005) 595–608
European Journal of Cell Biology
www.elsevier.de/ejcb

GFP-FABD2 fusion construct allows in vivo visualization of the dynamic actin cytoskeleton in all cells of *Arabidopsis* seedlings

Boris Voigt[a], Antonius C.J. Timmers[b], Jozef Šamaj[a,c], Jens Müller[a], František Baluška[a], Diedrik Menzel[a,*]

[a]*Department of Plant Cell Biology, Institute of Cellular and Molecular Botany, Rheinische Friedrich-Wilhelms-University of Bonn, Kirschallee 1, D-53115 Bonn, Germany*
[b]*Laboratoire Interactions Plantes-Microorganismes, INRA/CNRS, Chemin de Borderouge, F-31326 Castanet-Tolosan, France*
[c]*Institute of Plant Genetics and Biotechnology, Slovak Academy of Sciences, Akademická 2, SK-95007 Nitra, Slovakia*

Received 3 November 2004; accepted 4 November 2004

Abstract

In vivo visualization of filamentous actin in all cells of *Arabidopsis thaliana* seedlings is essential for understanding the numerous roles of the actin cytoskeleton in diverse processes of cell differentiation. A previously introduced reporter construct based on the actin-binding domain of mouse talin proved to be useful for unravelling some of these aspects in cell layers close to the organ surface. However, cells more deeply embedded, especially stelar cells active in polar transport of auxin, show either diffuse or no fluorescence at all due to the lack of expression of the fusion protein. The same problem is encountered in the root meristem. Recently introduced actin reporters based on fusions between *A. thaliana* fimbrin 1 and GFP gave brilliant results in organs from the root differentiation zone upwards to the leaves, however failed to depict the filamentous actin cytoskeleton in the transition zone of the root, in the apical meristem and the root cap. To overcome these problems, we have prepared new transgenic lines for the visualization of F-actin in vivo. We report here that a construct consisting of GFP fused to the C-terminal half of *A. thaliana* fimbrin 1 reveals dynamic arrays of F-actin in all cells of stably transformed *A. thaliana* seedlings.

Keywords: Actin cytoskeleton; *Arabidopsis thaliana*; Fimbrin; GFP

Introduction

In vivo visualization of the actin cytoskeleton is critical due to the extreme dynamism of actin filaments. Over a long time, concerns have been discussed as to whether chemical fixation sufficiently preserves the more dynamic F-actin populations in plant cells. There has been some expectations that this problem may be overcome by the recently established GFP-reporter technology. In fact, data obtained with the GFP-talin (GFP-mTn) construct (Kost et al., 1998, 2000) have been encouraging. As a consequence this new construct is widely used and numerous studies have been published on epidermal cells, especially on trichomes of wild-type and diverse mutants of *Arabidopsis thaliana* (El-Din El-Assal et al., 2004; Jedd and Chua, 2002; Li et al., 2003; Mathur et al., 1999, 2002, 2003a,b). However, as it has turned out, there is some constraint

*Corresponding author. Tel.: +49 228 73 5999; fax: +49 228 73 9004.
E-mail address: dmenzel@uni-bonn.de (D. Menzel).

0171-9335/$ - see front matter © 2005 Elsevier GmbH. All rights reserved.
doi:10.1016/j.ejcb.2004.11.011

in the use of this construct for in vivo analysis of root apex cells as well as of stelar cells localized deeper in plant organs. These tissues are of particular interest because they are essential for the polar transport of auxin, which is mediated by the putative auxin efflux carriers PIN1, PIN3 and PIN4 (Friml et al., 2002a,b; Geldner et al., 2001; Grebe et al., 2002; Willemsen et al., 2003) and which is partially dependent on the intact actin cytoskeleton (Muday, 2000; Muday et al., 2000; Sun et al., 2004). Similarly, elucidation of other roles of F-actin in pericycle and stele, including initiation of lateral roots, are critically dependent on in vivo visualization of dynamic arrays of F-actin. However, this has been difficult due to the fact that these cells are localized more deeply in the root body. Therefore, development of an improved reporter for in vivo visualization of F-actin in plants is essential for understanding how the actin cytoskeleton dynamically interacts with components of polar transport of auxin within the root stele.

Using Steedman's wax-based immunolocalization technique, we have reported previously for maize root apices that stele cells are extremely rich in F-actin and accomplish dramatic reorganization of their actin filament system in the transition zone interpolated between meristem and the zone of rapid elongation (Baluška et al., 1997a, 2000). This reorganization of the actin cytoskeleton in cells of the transition zone encompasses dramatic accumulation of perinuclear F-actin elements which then organize into prominent bundles extending towards the non-growing but F-actin-rich end-poles (Baluška et al., 1997a, 2000). Depolymerization of F-actin with both cytochalasin D and latrunculin B prevented these cells from accomplishing cell elongation (Baluška et al., 2001a,b). Another controversial topic is the status of the actin cytoskeleton in root cap statocytes, which accomplish gravisensing within seconds of gravistimulation. Although F-actin is generally implicated in gravisensing, most attempts to visualize F-actin elements in these cells failed. The only report of distinct F-actin in root cap statocytes was based on the application of phalloidin before/during fixation of samples (Collings et al., 2001) which might result in aberrantly induced actin polymerization.

Answering these questions requires transgenic seedlings stably transformed with F-actin-specific GFP reporter constructs allowing in vivo visualization of the actin cytoskeleton in all cells of the root apex. As the GFP-mTn construct did not allow visualization of F-actin in most cells of the meristem and transition zone, we embarked on designing and testing other GFP constructs which might be helpful for in vivo visualization of F-actin. One of these constructs is GFP-FABD2, an N-terminal fusion of GFP to the C-terminal half of AtFim1 (aa 325–687), which includes the second actin-binding domain and the C-terminal end of *A. thaliana* fimbrin 1 (gift from David McCurdy). We have recently demonstrated the usefulness of this construct in a preliminary fashion in *Arabidosis* epidermal tissues (Ketelaar et al., 2004a) and it worked also quite well in tobacco protoplasts after subcloning into a different binary vector (Sheahan et al., 2004). Here we give a full account of the properties of this construct in *Arabidopsis* seedlings and compare it with other GFP-based actin reporter constructs from our and from other laboratories. We show that GFP-FABD2 is by far the best suited reporter for filamentous plant actin so far. In contrast to GFP-fusions with the complete sequence of AtFim1 (GFP-AtFim1), the C-terminal fusion to the first actin-binding domain of human plastin (Timmers et al., 2002), and the N-terminal fusion to the actin-binding domain of mouse talin (GFP-mTn), our new construct (GFP-FABD2) reports a very detailed image of the filamentous actin cytoskeleton in virtually all cell types of the *A. thaliana* seedling. In contrast to the recent report by Wang et al. (2004), who have examined the usefulness of several other GFP-fusion variants to *A. thaliana* fimbrin 1 as fluorescent reporters of the plant actin cytoskeleton, our construct gives a detailed representation of the actin cytoskeleton in the root transition zone, in the apical meristem and in the root cap. Therefore, the GFP-FABD2 fusion construct provides us with the unique opportunity to analyze the dynamic changes in the architecture of the root actin cytoskeleton in vivo in the course of organ development.

Materials and methods

Constructs

The coding region of AtFim1 (At4g26700) was amplified from pGEX-Fim1 (Kovar et al., 2000; McCurdy and Kim, 1998) by PCR using the following primers: 5′-GCACTAGTCTCATGAGTGGGTACGT-GGGTGTTGTCG-3′ and 5′- CGACTAGTTCATGA-CTTCGATGGATGCTTCCTCTGAG-3′. Underlined restriction enzyme sites, which had been added to the primers, were utilized to ligate the open reading frame to the SpeI site of pCATgfp (Reichel et al., 1996), resulting in pGFP-Fim1. In order to generate a construct containing the second actin-binding domain, pGFP-Fim1 was digested with BamHI and SpeI, the fragment recovered from an agarose gel and ligated in frame into a modified pCAT-GFP, resulting in pGFP-FABD2 (see also Ketelaar et al., 2004a). The stop codon of the GFP reading frame was removed by site-directed mutagenesis (Chameleon Mutagenesis Kit, Stratagene). The expression plasmid contained the 35S promoter of Cauliflower Mosaic Virus (CaMV) with a duplicated transcriptional enhancer, the Tobacco Etch Virus leader sequence functioning as a translational enhancer and the

polyadenylation signal of the CaMV 35S RNA. For the generation of stably transformed *A. thaliana* plants the expression cassettes were excised by SdaI and cloned into the PstI site of the binary vector pCB302 (Xiang et al., 1999). The binary vector constructs, pCB-GFP-Fim1 and pCB-GFP-FABD2, were introduced into *Agrobacterium tumefaciens* strain GV3101 (pMP90) by electroporation (Cangelosi et al., 1991). *A. thaliana* Col-0 plants were transformed by *A. tumefaciens* using the floral-dip method (Clough and Bent, 1998). Transformed plants (T1) were selected by screening for green fluorescent seedlings with a Leica MZ FL III fluorescence binocular equipped with a gfp3 emission filter (Leica). Fluorescent seedlings were transferred to soil and propagated for selfing. For microscopic analysis T3 and T4 plants were used. Transformed roots of *Medicago truncatula* cv. Jemalong were obtained using *A. rhizogenes* ARqua1 according to the protocol of Boisson-Dernier et al. (2001). About 3–6 weeks later, plants with transformed roots were put individually into square 12-cm plastic dishes (Greiner Labortechnik, Kremsmünster, Austria).

Growth conditions and media

All plants were grown at 22 °C at a 16-h day/8-h night cycle. For microscopy studies and measurements of *A. thaliana*, seedlings were grown on vertical Petri dishes containing one-half strength Murashige and Skoog salts with vitamins, 1% (w/v) sucrose and 0.4% (w/v) Phytagel (Sigma). Liquid culture medium had the same composition without Phytagel. *M. truncatula* were grown on Fahraeus medium containing 1% agar.

Sample preparation for microscopy

Transgenic seeds were plated on Petri dishes. The seedlings were grown for 4–7 days under standard conditions (see above). Seedlings were mounted in liquid medium between slide and coverslip seperated by a spacer and allowed to adjust in a humid chamber under standard growth conditions for at least 12 h before observation.

Microscopy

M. truncatula roots growing on agar were covered with bioFolie 25 (Sartorius AG, Vivascience Support Center, Göttingen, Germany) and observed with a LEICA TCS 4D confocal microscope (Leica, Wetzlar, Germany) using a 63 × water-immersion objective. *A. thaliana* samples were examined using a 40 × oil immersion lens under the confocal microscope equipped with an argon/krypton laser. GFP fluorescence was imaged using excitation with the 488-nm line of the argon/krypton laser and a 515-nm long pass or 530-nm band pass emission filter. Serial confocal optical sections were taken at different step sizes. Projections of serial confocal sections and contrast enhancement were done using image processing software (Scion Image; Scion Corporation; Photoshop, Adobe Systems Inc., Mountain View, CA, USA). For growth and curvature measurements, seedlings were observed directly on the Petri dishes with a 10 × lens mounted on an inverted Leica DMIRB microscope equipped with CCD camera, or the Petri dishes were placed on a standard PC scanner. Analysis and measurements were made with Image-Pro Plus 4.1 (Media Cybernetics, L.P.).

Results

GFP-FABD2 allows in vivo visualization of F-actin in all cell types

We have tested two different variants of GFP-fusion proteins based on *A. thaliana* fimbrin. The whole molecule fused to GFP and just the C-terminal actin-binding domain fused to the C-terminus of GFP. The resulting GFP-FABD2 (Ketelaar et al., 2004a) fusion protein allowed generation of transformed seedlings which had all cells labeled with the fluorescent F-actin reporter. Extensive arrays of longitudinal actin bundles and a dynamic network of actin filaments could be documented in elongated epidermal cells of the hypocotyl (Fig. 1A; Supplementary Movie 1). In trichomes of primary leaves, a prominent F-actin cage was present around the nucleus, and longitudinal filament bundles reached into the trichome tips (Fig. 1B, inset). Stomata cells showed thick filament bundles arranged in dense partially radial arrays throughout the cortex and a more prominent meshwork around the nucleus (Fig. 1C), similar to what has been shown previously (Kost et al., 2000).

In lateral root cap cells expressing GFP-FABD2 a system of long and thick F-actin bundles filled the cell cortex (Fig. 1D). Dense F-actin networks, reported in an earlier study (Collings et al., 2001), were absent from statocytes. Maybe due to the characteristics of the 35S promotor, the level of expression in the lateral cap was always higher than in statocyte cells. In single optical sections through the root cap, at the middle plane of the columella, just a diffuse, patchy pattern of GFP-FABD2 was visible (Fig. 1E, stars). In this section, the lateral root cap cells (Fig. 1E, diamonds) show a lower overall signal due to the fact that the thick filaments at the cell cortex were cut perpendicularly. Again, in contrast to the findings of Collings et al. (2001) who examined other plant species, no distinct F-actin bundles could be observed in the statocytes of transgenic *A. thaliana*

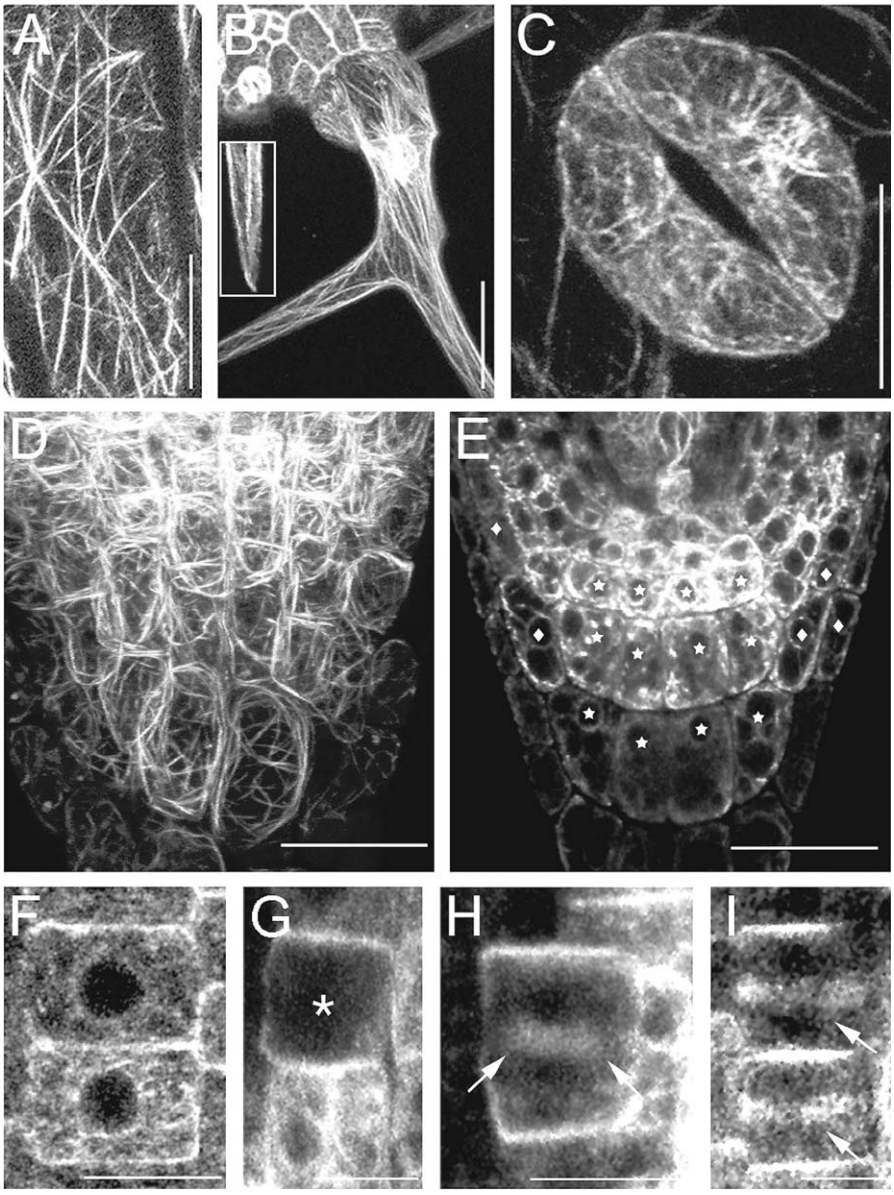

Fig. 1. In vivo visualization of F-actin using GFP-FABD2 in different cell types of Arabidopsis. (A) Epidermal cell of the hypocotyl. (B) Trichome, inset represents a tip of a trichome. (C) Guard cells. (D) Lateral root cap cells with cortical F-actin bundles. (E) Single optical section through the root cap. Columella cells (stars) and lateral root cap cells (diamonds) showing different actin states. (F) Interphase cell of the meristem. (G) Mitotic cell, with F-actin-depleted zone (asterisk). (H and I) Phragmoplast F-actin at different stages of cytokinesis (arrows). Images A–D are projections of 6–20, images F–I of 2–4 confocal optical sections. Bars A, D, E = 20 μm; B = 50 μm; C, F−I = 10 μm.

plants. In the meristematic zone of the root, interphase cells exhibit very fine and highly dynamic meshworks without any thicker bundles of F-actin (Fig. 1F). Mitotic cells have a F-actin-depleted zone (Fig. 1G, star) at around the equator, whereas F-actin accumulates at the plasma membrane which is facing the spindle poles (Fig. 1G). During cytokinesis this overall actin polarity is still maintained. Fig. 1H shows a cytokinetic cell with strongly labeled cross-walls and F-actin depleted at the lateral plasma membrane areas. The phragmoplast F-actin could be observed at different stages (Fig. 1H and I, arrows) of cytokinesis.

Moving towards the root base, the transition zone exhibits a very special actin pattern. Fig. 2A gives an overview of developmental stages in the cortex cell layer from apical meristem to elongation zone, with the transition zone interpolated in-between them. While dividing cortex cells of the meristem show fine meshworks throughout their cytoplasm, F-actin of the cortex cells at the transition zone become bundled, enclosing

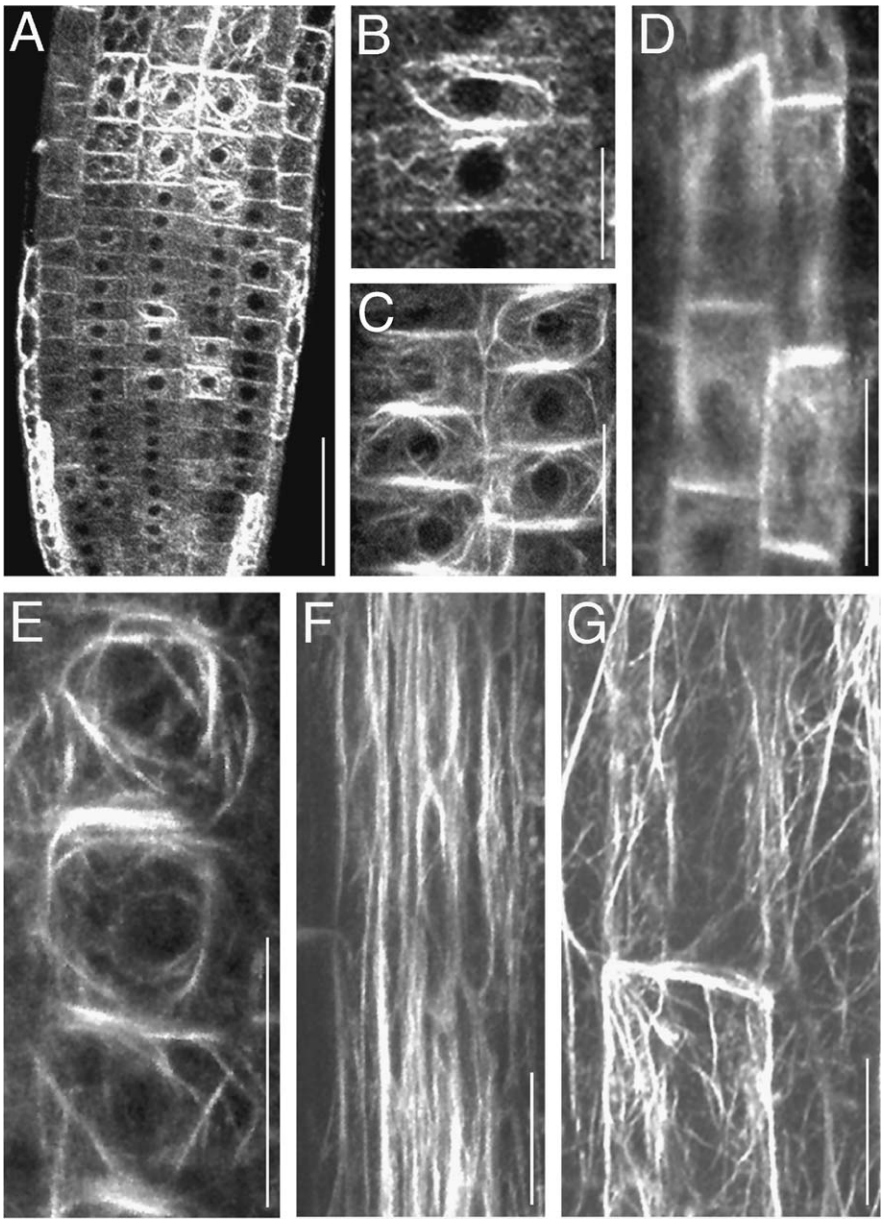

Fig. 2. In vivo visualization of F-actin using GFP-FABD2 in the transition and elongation zone of *Arabidopsis* roots. (A) Overview from meristem to early elongation zone within root cortex layer. (B) Higher magnification of cells entering the transition zone. (C and E) Cortex cells leaving the transition zone and starting with elongation. (D) Endodermis cells within the transition zone. (F) Elongated endodermis cells. (G) Elongated cortex cells. Images A and B are single, images C–G are projections of 4–10 confocal optical sections. Bars A = 50 μm; B−G = 20 μm.

the nucleus and attaching to the F-actin-rich cross walls. These F-actin bundles appear first when the cortex cells cease divisions and enter the transition zone (Fig. 2B). Later on, when elongation of the cortex cells starts, the F-actin bundles around the nucleus as well as the labeling at the cross walls get more prominent (Fig. 2C and E). Finally, in fully elongated cortex root cells, mostly longitudinal filament bundles as well as a fine and highly dynamic network of F-actin occur at the cortex cells (Fig. 2G).

Nearly the same pattern was observed in cells of the endodermis (Fig. 2D and F). Non-elongated endodermis cells have a strong signal at the cross walls with some actin stretches around the nucleus (Fig. 2D, poorly resolved due to depth of focal plane). Whereas fully elongated endodermis cells show no strong signal at cross walls. Instead, longitudinally filament bundles run throughout the entire length of the cell (Fig. 2F).

The actin cytoskeleton is very important for polar growth, which occurs in tip-growing root hairs. At every

stage of the root hair development the actin cytoskeleton could be observed properly (Fig. 3). In early root hair bulges, an extensive meshwork of F-actin patches and bundles was present at the cell cortex (Fig. 3A). At a somewhat later stage, when the root hair began to grow by tip growth, filament bundles still extend in the direction of the tip and then disperse into a very fine and dynamic meshwork at the very apex (Fig. 3B). The same pattern of organization was seen at the tip of fast growing root hairs (Fig. 3C; Supplementary Movie 2). Due to their motile activity, small bundles or possibly single actin filaments right at the tip, are just about visible in movies. Fig. 3D is an image taken from a low-resolution, but fast scanned time-lapse series. Small filaments moving around the tip of the root hair are slightly visible. Actin patches (Fig. 3D, arrows) are always associated with the tip region of growing hairs. Full grown root hairs show big filament bundles throughout the whole cell merging right into the tip and back (Fig. 3E). To test, whether the fusion construct somehow has a stabilizing effect on F-actin, we applied the F-actin-depolymerizing drug latrunculin B (LatB). Fig. 3F–H show root tricho- and atrichoblast cells before (Fig. 3F) and after 4 min of 400 nM LatB

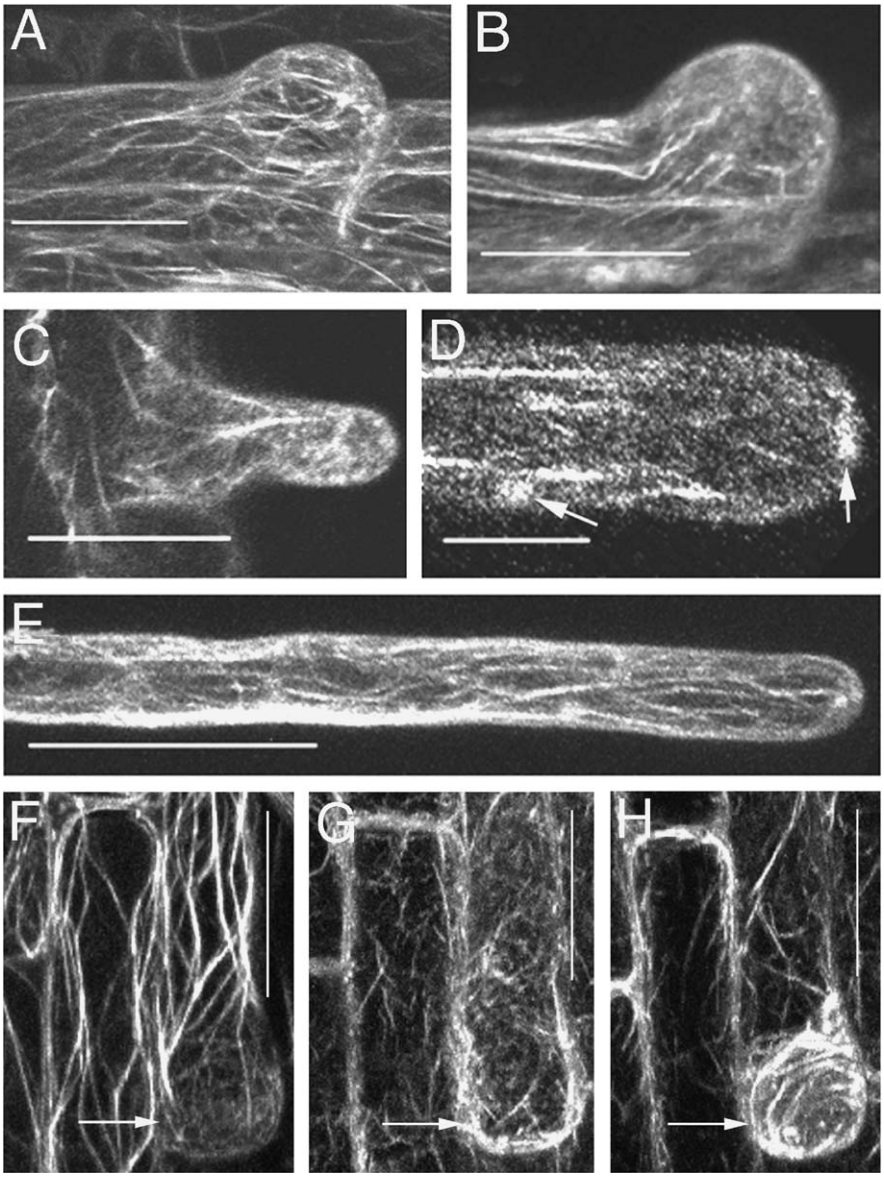

Fig. 3. In vivo visualization of F-actin using GFP-FABD2 in all stages of root hair development. (A) Early bulge. (B) Late bulge with beginning tip growth. (C) Young growing root hair. (D) Tip of fast growing root hair; arrows indicate actin patches. (E) Growth-terminated root hair. (F) Root epidermal cells with outgrowing bulge (arrow). (G) Same cells as in (F) after 4 min of 400 nM LatB. (H) Same cells after 25 min LatB and 50 min wash out. Images A, B, E–H are projections of 6–15 confocal optical sections. Images C and D are single confocal optical sections. Bars A–D, F−H = 20 μm; E = 25 μm.

treatment (Fig. 3G). Fig. 3H shows the same cells after 25 min 400 nM LatB treatment and following 50 min of washing out. It is obvious that the prominent as well as the fine F-actin depolymerizes to shorter F-actin filaments or even to G-actin. It seems that the depolymerized actin becomes a bit accumulated in the very tip of the outgrowing root hair bulge (Fig. 3G, arrow). After LatB was washed out, thicker and more densely packed F-actin filaments were rebuilt and appeared at the outgrowing root hair tip (Fig. 3H).

Comparison with other in vivo F-actin markers

Examination of transgenic *A. thaliana* seedlings transformed with GFP-Fim1 (GFP-fused to the N-terminus of the entire fimbrin 1 molecule) showed unusual patterns of F-actin distributions in epidermal cells of the hypocotyl (Fig. 4A). The cortical actin cytoskeleton appeared as a dense, interwoven meshwork without any preferential orientation. In epidermal cells (Fig. 4B) of the root, however, there were almost no filamentous structures visible except for a diffuse signal in cytoplasmic strands. The same was true for epidermis and cortex cells in the transition zone (Fig. 4C).

Transgenic *M. truncatula* roots transformed with plastin-GFP (GFP-fused to the C-terminus of a truncated human T-plastin, Timmers et al., 2002) showed yet another pattern of the actin cytoskeleton. In root epidermis cells, thick, filamentous interwoven structures formed a coarse actin network and the nuclei were always prominently labeled (Fig. 5A). A closer look at root hairs revealed that only occasionally F-actin bundles were visible, whereas most of the cytoplasm was filled with a diffuse signal (Fig. 5B) which could correspond to the endoplasmic reticulum rather than to the actin cytoskeleton.

Seedlings which express GFP-mTn (GFP-fused to the N-terminus of mouse talin, Kost et al., 1998, 2000) showed a similar kind of F-actin arrangements as that seen with GFP-FABD2 in most cell types. However, in lateral root cap cells the very prominent filamentous actin network seen with GFP-FABD2 (Fig. 1D) was not visible, instead, just a diffuse cytoplasmic signal occurred (Fig. 5C). Nearly the same situation we found in the root cap statocytes (Fig. 5C compare to Fig. 1E). On the other hand, in root epidermis cells the F-actin was very much like that seen after labeling with GFP-FABD2, i.e., exhibiting big longitudinal filaments and a randomly arranged fine F-actin network (Fig. 5D). In addition, we always found a strong background of GFP signal in the cytoplasm and always a labeling of the nuclei (Fig. 5E). The same pattern could be observed in growing root hairs, where nearly the complete root hair shows a diffuse signal with some prominent F-actin bundles included (Fig. 5F). We could not

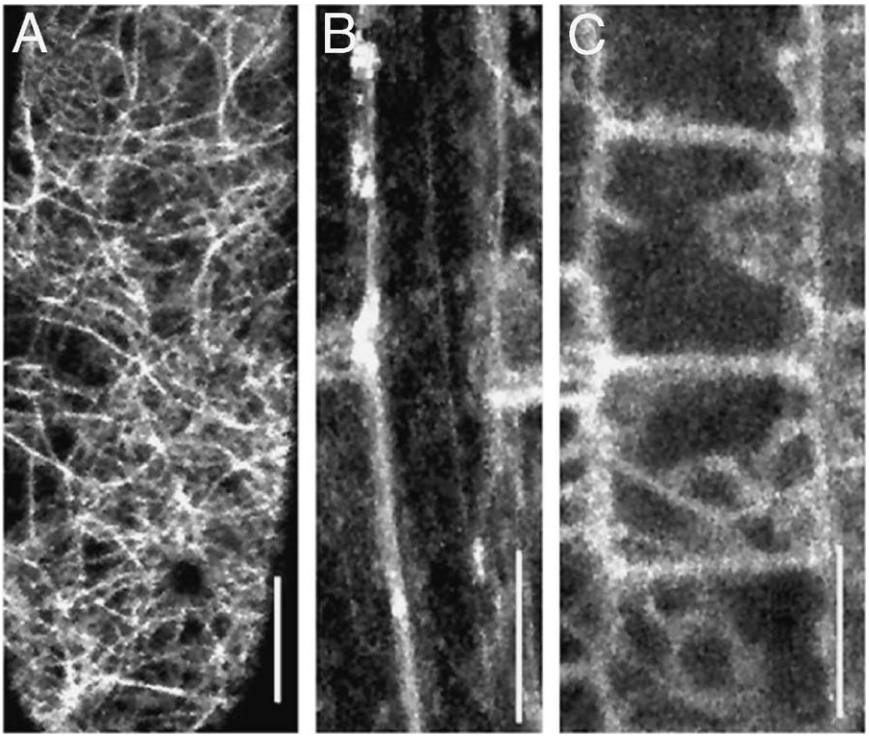

Fig. 4. In vivo visualization of GFP-Fim1-labeled structures in different cells of *Arabidopsis*. (A) Hypocotyl cell. (B) Root epidermal cell. (C) Cortex cells within the transition zone of the root apex. Images A and B are projections of 4–5 confocal optical sections, C is a single confocal optical section. Bars A = 10 μm; B, C = 20 μm.

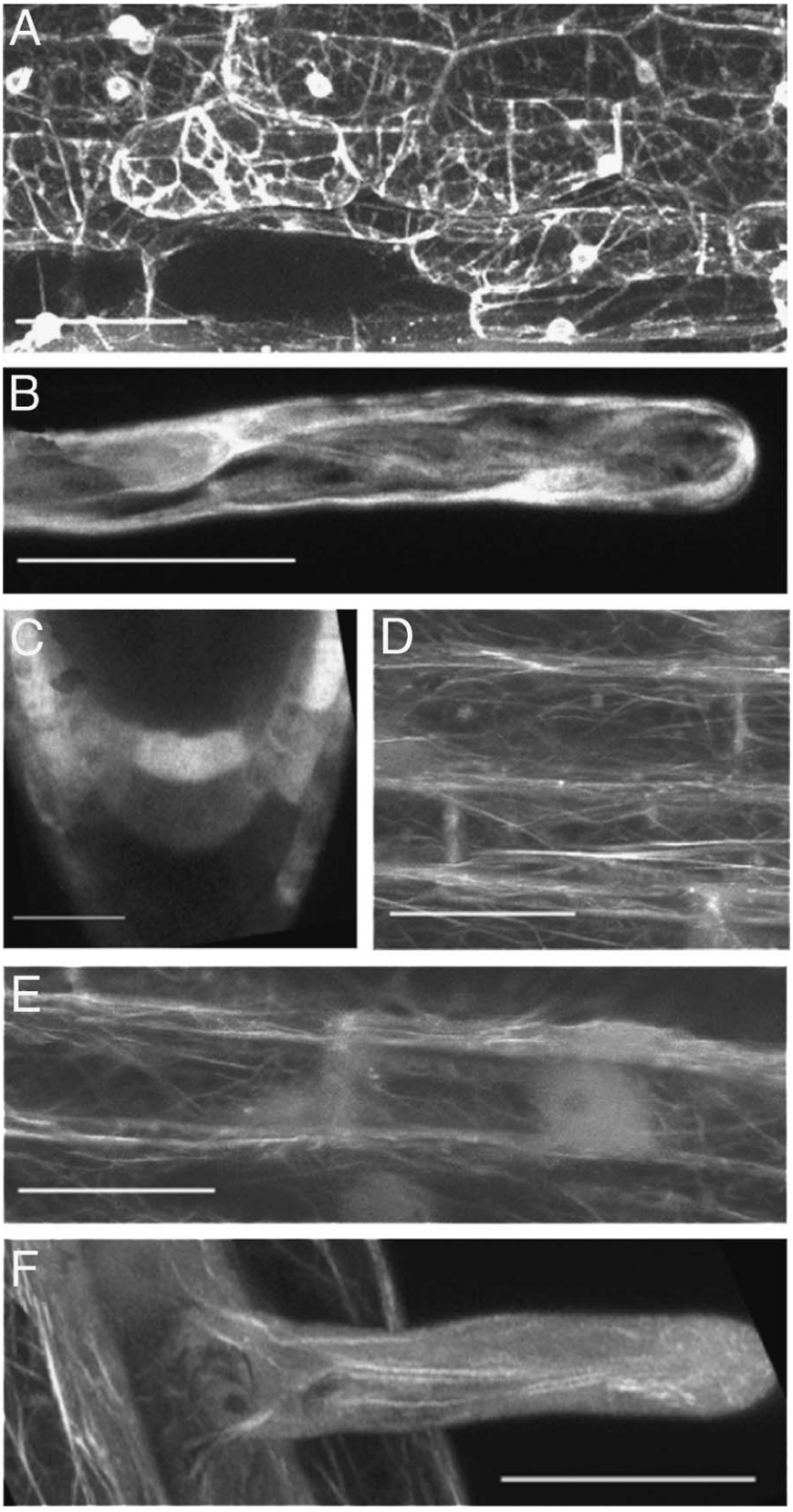

Fig. 5. Plastin-GFP and GFP-mTn expressed in *M. truncatula* and *A. thaliana*. (A) Plastin-GFP labeled thick filament bundles and the nuclei of *Medicago* root epidermal cells. (B) A diffuse signal of plastin-GFP is detectable in *Medicago* root hair. (C) GFP-mTn transgenic *Arabidopsis* show weak and diffuse signals in lateral root cap cells and statocytes. (D and E) GFP-mTn labeled filament bundles, fine F-actin networks and nuclei in root epidermal cells. (F) GFP-mTn root hairs showed few actin bundles and a huge diffuse background. Images A, B and D–F are projections of 10–30 confocal optical sections, C is a single confocal optical section. Bars = 25 μm.

compare the actin states in the other parts of GFP-mTn seedlings such as cortex, endodermis, and stele cells of the transition zone due to the fact that there was no signal detectable. The same is true for the entire meristem.

Arabidopsis stably transformed with GFP-FABD2 show normal growth in response to light, darkness and gravity

In order to rule out that the GFP-FABD2 construct interferes with endogenous fimbrin-based processes, we determined the growth rates of root hairs, as well as the responses of roots to gravistimulation and hypocotyls to darkness (Table 1A–C; Fig. 6). All these parameters showed values corresponding well to those found in wild-type *A. thaliana* seedlings. These data clearly indicate that the GFP-FABD2 lines are well suited for physiological experiments, including photo- and gravitropic responses which both depend on the polar transport of auxin. In all other situations tested, we did not score any significant deviation of growth values from those found in wild-type plants. Moreover, we did not detect any phenotypic changes in the GFP-FABD2 seedlings. In comparison to wild-type and GFP-FABD2 seedlings, the GFP-mTn seedlings showed a slightly decreased hypocotyl growth and a significantly slower gravitropic response (Table 1A–C, Fig. 6).

Discussion

A. thaliana seedlings stably transformed with the GFP-FABD2 fusion construct provide us with the unique opportunity to study the actin cytoskeleton in vivo in all cell types throughout the plant body in the course of organ development. In addition to the already well characterized trichomes, we are now in the position to answer critical questions related to in vivo roles of the actin cytoskeleton within cells of the root cap, meristem, transition zone, root hairs, as well as diverse stelar cell types. In particular, we can study the involvement of the actin cytoskeleton in the redistribution of auxin throughout the root apices which is closely related to vesicle recycling (Baluška et al., 2003; Geldner et al., 2003; Muday et al., 2000). Furthermore, the GFP-FABD2 construct is also suitable for visualization of the actin cytoskeleton in other monocot and dicot plant species including *Allium cepa, Medicago truncatula*, *Vicia faba,* and tobacco BY-2 suspension cells (our unpublished data).

As recently reported by Wang et al. (2004) the BD1/2-GFP construct also based on *A. thaliana* fimbrin 1 is well suited to represent the actin cytoskeleton in great detail in a similar fashion as GFP-FABD2 in cells of the elongation zone, of the root upward to the hypocotyl and to the leaves. However, as far as the lower portions of the root, including the transition zone, the apical meristem and the root cap, are concerned, BD1/2-GFP and all other variants tested by Wang et al. (2004) have reported mainly a diffuse cytoplasm-based distribution of actin, which is not consistent with our present view of the actin cytoskeleton in these areas of the root, even though some controversy remains (see below). This gap in our capablility to observe in vivo the architecture and dynamics of the actin cytoskeleton in the proximal regions of the root organ has now been closed with the availability of the GFP-FABD2 transgenic *A. thaliana* line.

GFP-mTn transgenic lines also have some shortcomings as we report here. This is in agreement with reports from other labs (Ketelaar et al., 2004b; Wang et al., 2004). For instance, GFP-mTn is not useful for studies on the redistributions of F-actin in dividing cells because meristematic cells at the root apex are either devoid of reporter gene expression or the expressed fusion protein is diffusely distributed in cells of that developmental stage. In contrast, the dividing cells of GFP-FABD2-transformed root apices had a high enough level of expression allowing the in vivo tracking of F-actin redistribution throughout mitosis and cytokinesis in the spatial context of the entire tissue. In accordance with previously published data on dividing root apex cells obtained using Steedman's wax embedding technique (Baluška et al., 1997a), interphase cells show meshworks of F-actin arrays encasing the central nucleus and connecting it to the plasma membrane, without any distinct polarity of actin-enriched domains. However, as soon as cells enter mitosis, they disassemble and deplete F-actin in the central part of the cell and accumulate dense F-actin layers under the plasma membrane domains facing the spindle poles, whereas the lateral plasma membrane domains, which in preprophase are occupied by the preprophase band of microtubules are depleted in F-actin (Baluška et al., 1997a, 2000; see also Fig. 1F–H). This rapid and dramatic redistribution of the actin cytoskeleton suggests that meristematic cells express their inherent polarity along the root axis even though it becomes structurally manifested only in mitotic and cytokinetic cells. During cytokinesis, parent cells maintain the distribution of F-actin-enriched and -depleted domains as was described for mitosis. In addition, they assemble F-actin also in microtubule-dependent phragmoplasts navigating cell plate vesicles into mid-line destined to be the future new cell wall between the daughter cells. F-actin localization by GFP-reporters in structures resembling a phragmoplast has previously been reported by Wang et al. (2004).

With the GFP-FABD2 transgenic line we have the ideal opportunity to re-investigate in vivo the

Table 1. Root hair growth, hypocotyl length and gravitropic response of wild-type and transformed *Arabidopsis* seedlings

A	Root hair growth speed (μm/min)	Root hair average growth speed (μm/min)	SD	SE
Wild-type ($n = 34$)	0.7–1.76	1.39	0.29	0.05
GFP-FABD2 ($n = 29$)	1.11–2.04	1.62	0.23	0.04
GFP-mTn ($n = 33$)	0.96–2.08	1.59	0.28	0.05
B	Hypocotyl length 1 day after germination in mm (SE)	Hypocotyl length 7 days after germination in mm (SE)	Average growth rates between 2 and 5 days after germination in mm/24 h	
Wild-type ($n = 33$)	1.65 (0.10)	19.03 (0.28)	3.6	
GFP-FABD2 ($n = 45$)	1.88 (0.07)	20.05 (0.24)	3.5	
GFP-mTn ($n = 7$)	1.26 (0.14)	15.25 (0.66)	3.1	
C	Average root curvature 18 h after re-orientation, degrees (SE)		p-value of ANOVA against wild type	
Wild-type ($n = 22$)	76.35 (2.64)			
GFP-FABD2 ($n = 28$)	79.50 (1.62)		0.316	
GFP-mTn ($n = 23$)	59.87 (2.72)		0.000	

(A) The growth speed of root hairs was measured for 30 min only on fast growing hairs longer than 20 μm of seedlings grown on top of vertical Petri dishes. The growth rates were calculated to μm/min and then averaged. The GFP-FABD2 and GFP-mTn transgenic lines show a slightly increased growth speed compared to wild-type root hairs. (B) The hypocotyl length of etiolated seedlings was measured each day until 7 days after germination. There was almost no difference of the growth speed of GFP-FABD2 (3.5 mm/24 h) compared to wild type (3.6 mm/24 h), in contrast to GFP-mTn seedlings, which had a decreased hypocotyl growth speed (3.1 mm/24 h). (C) Seedlings were germinated in the dark and grown vertically for 2 days before the plates were re-oriented by 90°. The angle of the root curvature was measured 18 h after re-orientation. GFP-FABD2 and wild-type seedlings show no significant (ANOVA, $p = 0.316$) difference in the graviresponse, whereas GFP-mTn seedlings exhibited a significant (ANOVA, $p = 0.000$) slower bending of the root.

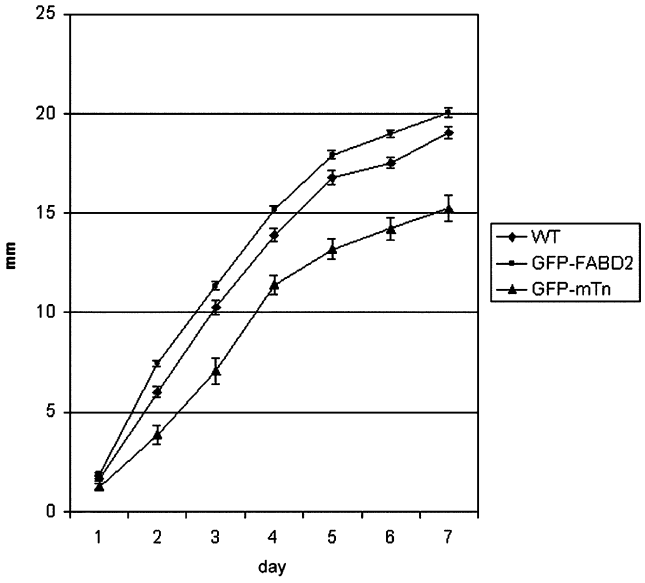

Fig. 6. Hypocotyl length of etiolated wild-type (WT), GFP-FABD2 and GFP-mTn *Arabidopsis* seedlings measured each day until 7 days after germination on vertical Petri dishes. WT and GFP-FABD2 seedlings show no signifcant difference in the hypocotyl growth speed, whereas GFP-mTn seedlings exhibit a slower growth speed (see also Table 1B).

major developmental switch occurring in the F-actin distribution of cells advancing from the meristem to the elongation zone with the transition zone interpolated in between (Baluška et al., 1997a, 2000, 2001a,b). Our previous immunofluorescence study, using Steedman's wax sectioning, revealed that cells in the transition zone assemble prominent actin bundles which are initiated at the nuclear surface and remain in lateral contact with the centrally positioned nuclei. Subsequently, these actin bundles extend towards the non-growing cross walls harbouring numerous plasmodesmata and align laterally along their plasma membrane (Baluška et al., 1997a). We have hypothesized that both the nuclear envelope as well as the plasma membrane domains underneath the cross walls act as some kind of actin filament-organizing centers (AFOCs) which would define the structural polarity of these cells as they are preparing for rapid elongation (Baluška et al., 2000; Volkmann and Baluška, 1999). Conceivably, there has always been some concern on the reliability of these observations because the specimens had to be chemically fixed and fixation, being a rather slow process, might allow some aberrant redistributions of actin filaments. Here, we show convincingly that living root cells of *A. thaliana* exhibit exactly the same pattern of F-actin distribution and perform the same sequence of restructuring, which had been deduced from the fixed material, i.e., actin filaments start bundling at lateral domains of the nuclear surface and then progressively protrude out towards the cross walls at the cell poles. Because GFP-mTn roots do not show F-actin elements in cells of the transition zone, and the recent study by Wang et al. (2004) gives no account of F-actin redistributions in this area of the root, we document this phenomenon here for the first time in living root cells. Moreover, our pharmacological approaches revealed that this unique arrangement of the actin cytoskeleton plays a crucial role in the onset of rapid cell elongation (Baluška et al., 1997a, 2001a; Volkmann and Baluška, 1999). Such a critical role of the dynamic rearrangement of the actin cytoskeleton at this developmental stage has meanwhile also been confirmed using genetic approaches (Barrero et al., 2002, 2003; Dong et al., 2001; Gilliland et al., 2002; Nishimura et al., 2003; Ramachandran et al., 2000; Ringli et al., 2002).

The possibility of visualizing F-actin in cells of the transition zone is fundamental also for understanding the potential role of the actin cytoskeleton in gravitropism of the root because the graviresponse is initiated in this particular zone of the root via differential speed with which cells traverse this developmental stage and begin to elongate (Baluška et al., 1996, 2001a). Here we report that root growth and its graviresponse in GFP-FABD2 transgenic seedlings is very similar to wild-type plants. This is in contrast to GFP-mTn seedlings, which have a slightly decreased hypocotyl growth and a significantly slower gravitropic response. Moreover, etiolated hypocotyls undergo rapid growth in both wild-type and GFP-FABD2 plants. Last but not least, root hairs are well-known to be extremely sensitive to environmental perturbations resulting in the cessation of tip growth. This sensing of the environment involves the actin cytoskeleton and signaling components such as mitogen-activated protein kinases (Šamaj et al., 2002, 2004). Importantly, root hairs of GFP-FABD2 transgenic seedlings show growth rates slightly exceeding those scored for root hairs of wild-type roots. Moreover, in contrast to GFP-mTn root hairs showing predominantly a diffuse signal at root hair apices, GFP-FABD2 root hairs reveal dynamic populations of thin, presumably unbundled F-actin protruding up to the very tips of growing root hairs. Besides dynamic F-actin elements, we scored also motile patches of F-actin moving vigorously within apices of growing tips. Elucidating the role of these structures will require further studies but our preliminary data suggest that they are associated with early endosomes (Voigt et al., 2005). Jasplakinolide is a potent drug inducing overpolymerization of F-actin (Bubb et al., 2000; Šamaj et al., 2002; Sawitzky et al., 1999) and its application to root hairs expressing GFP-FABD2 construct induces rapid transformation of dynamic F-actin elements and patches into large and thick spindle-shaped aggregates. In contrast, latrunculin B at concentrations of 400 nM results in a complete, but reversible breakdown of the GFP-FABD2-labeled actin

cytoskeleton in root hairs as well as in cells of the root body.

By employing the GFP-FABD2 plants, we can now re-address the controversial issue of the state of the actin cytoskeleton in root cap cells, especially in the gravi-sensing statocytes positioned in the middle part of root caps, which has previously been studied by using fluorochrome-conjugated phalloidin (Collings et al., 2001). Filamentous actin structures seen in this study can certainly be taken as an indication for the presence of actin; however, due to the filament-stabilizing properties of phalloidin, the status of the actin cytoskeleton in these cells still remains controversial. Root cap statocytes are equipped with large amyloplasts which sediment towards their physical bottom in a process which is counteracted by residual actomyosin-based forces (Volkmann and Baluška, 1999). Weak actomyosin forces combined by the absence of robust cytoskeletal elements which would trap and restrain them in the deeper cytoplasm, all this should allow large and heavy amyloplasts to sediment along the gravity vector (Baluška et al., 1997b; Baluška and Hasenstein, 1997). Our present data provide in vivo confirmation of the absence of robust F-actin bundles within root cap statocytes which are otherwise assembling in all other postmitotic root cells and faithfully reported by GFP-FABD2.

Acknowledgement

We thank D. McCurdy for the cDNA of AtFim1, G. Jach for the pCATgfp vector and J. Mathur for providing us with transgenic GFP-mTn seeds. This work was partially supported by EU Research Training Network TIPNET (project HPRN-CT-2002-00265) obtained from Brussels, Belgium.

Appendix A. Supplementary materials

The online version of this article contains additional supplementary data. Please visit doi:10.1016/j.ejcb.2004.11.011.

References

Baluška, F., Hasenstein, K.H., 1997. Root cytoskeleton: its role in perception of and response to gravity. Planta 203, S69–S78.

Baluška, F., Volkmann, D., Barlow, P.W., 1996. Specialized zones of development in roots: view from the cellular level. Plant Physiol. 112, 3–4.

Baluška, F., Vitha, S., Barlow, P.W., Volkmann, D., 1997a. Rearrangements of F-actin arrays in growing cells of intact maize root apex tissues: a major developmental switch occurs in the postmitotic transition region. Eur. J. Cell Biol. 72, 113–121.

Baluška, F., Kreibaum, A., Vitha, S., Parker, J.S., Barlow, P.W., Sievers, A., 1997b. Central root cap cells are depleted of endoplasmic microtubules and actin microfilament bundles: implications for their role as gravity-sensing statocytes. Protoplasma 196, 212–223.

Baluška, F., Barlow, P.W., Volkmann, D., 2000. Actin and myosin VIII in developing root cells. In: Staiger, C.J., Baluška, F., Volkmann, D., Barlow, P.W. (Eds.), Actin: A Dynamic Framework for Multiple Plant Cell Functions. Kluwer Academic Publishers, Dordrecht, The Netherlands, pp. 457–476.

Baluška, F., Jasik, J., Edelmann, H.G., Salajova, T., Volkmann, D., 2001a. Latrunculin B-induced plant dwarfism: Plant cell elongation is F-actin-dependent. Dev. Biol. 231, 113–124.

Baluška, F., Busti, E., Dolfini, S., Gavazzi, G., Volkmann, D., 2001b. Lilliputian mutant of maize lacks cell elongation and shows defects in organization of actin cytoskeleton. Dev. Biol. 236, 478–491.

Baluška, F., Šamaj, J., Menzel, D., 2003. Polar transport of auxin: carrier-mediated flux across the plasma membrane or neurotransmitter-like secretion? Trends Cell Biol. 13, 282–285.

Barrero, R.A., Umeda, M., Yamamura, S., Uchimiya, H., 2002. *Arabidopsis* CAP regulates the actin cytoskeleton necessary for plant cell elongation and division. Plant Cell 14, 149–163.

Barrero, R.A., Umeda, M., Yamamura, S., Uchimiya, H., 2003. Over-expression of *Arabidopsis* CAP causes decreased cell expansion leading to organ size reduction in transgenic tobacco plants. Ann. Bot. 91, 599–603.

Boisson-Dernier, A., Chabaud, M., Garcia, F., Becard, G., Rosenberg, C., Barker, D.G., 2001. *Agrobacterium rhizogenes*-transformed roots of *Medicago truncatula* for the study of nitrogen-fixing and endomycorrhizal symbiotic associations. Mol. Plant Microb. Interact. 14, 695–700.

Bubb, M.R., Spector, I., Beyer, B.B., Fosen, K.M., 2000. Effects of jasplakinolide on the kinetics of actin polymerization. An explanation for certain in vivo observations. J. Biol. Chem. 275, 5163–5170.

Cangelosi, G.A., Best, E.A., Martinetti, G., Nester, E.W., 1991. Genetic analysis of *Agrobacterium*. Methods Enzymol. 204, 384–397.

Clough, S.J., Bent, A.F., 1998. Floral dip: a simplified method for *Agrobacterium*-mediated transformation of *Arabidopsis thaliana*. Plant J. 16, 735–743.

Collings, D.A., Zsuppan, G., Allen, N.S., Blancaflor, E.B., 2001. Demonstration of prominent actin filaments in the root columella. Planta 212, 392–403.

Dong, C.-H., Xia, G.-X., Hong, Y., Ramachandran, S., Kost, B., Chua, N.-H., 2001. ADF proteins are involved in the control of flowering and regulate F-actin organization, cell expansion, and organ growth in *Arabidopsis*. Plant Cell 13, 1333–1346.

El-Din El-Assal, S., Le, J., Basu, D., Mallery, E.L., Szymanski, D.B., 2004. DISTORTED2 encodes an ARPC2

subunit of the putative *Arabidopsis* ARP2/3 complex. Plant J. 38, 526–538.

Friml, J., Benkova, E., Blilou, I., Wisniewska, J., Hamann, T., Ljung, K., Woody, S., Sandberg, G., Scheres, B., Jürgens, G., Palme, K., 2002a. AtPIN4 mediates sink-driven auxin gradients and root patterning in *Arabidopsis*. Cell 108, 661–673.

Friml, J., Wisniewska, J., Benkova, E., Mendgen, K., Palme, K., 2002b. Lateral relocation of auxin efflux regulator PIN3 mediates tropism in *Arabidopsis*. Nature 415, 806–809.

Geldner, N., Friml, J., Stierhof, Y.D., Jürgens, G., Palme, K., 2001. Auxin transport inhibitors block PIN1 cycling and vesicle trafficking. Nature 413, 425–428.

Geldner, N., Anders, N., Wolters, H., Keicher, J., Kornberger, W., Muller, P., Delbarre, A., Ueda, T., Nakano, A., Jürgens, G., 2003. The *Arabidopsis* GNOM ARF-GEF mediates endosomal recycling, auxin transport, and auxin-dependent plant growth. Cell 112, 219–230.

Gilliland, L.U., Kandasamy, M.K., Pawloski, L.C., Meagher, R.B., 2002. Both vegetative and reproductive actin isovariants complement the stunted root hair phenotype of the *Arabidopsis* act2-1 mutation. Plant Physiol. 130, 2199–2209.

Grebe, M., Friml, J., Swarup, R., Ljung, K., Sandberg, G., Terlou, M., Palme, K., Bennett, M.J., Scheres, B., 2002. Cell polarity signaling in *Arabidopsis* involves a BFA-sensitive auxin influx pathway. Curr. Biol. 12, 329–334.

Jedd, G., Chua, N.-H., 2002. Visualization of peroxisomes in living plant cells reveals acto-myosin-dependent cytoplasmic streaming and peroxisome budding. Plant Cell Physiol. 43, 384–392.

Ketelaar, T., Allwood, E.G., Anthony, R., Voigt, B., Menzel, D., Hussey, P.J., 2004a. The actin-interacting protein AIP1 is essential for actin organization and plant development. Curr. Biol. 14, 145–149.

Ketelaar, T., Anthony, R.G., Hussey, P.J., 2004b. Green fluorescent protein-m talin causes defects in actin organization and cell expansion in *Arabidopsis* and inhibits actin depolymerizing factor's actin depolymerizing activity in vitro. Plant Physiol. 136, 3990–3998.

Kost, B., Spielhofer, P., Chua, N.-H., 1998. A GFP-mouse talin fusion protein labels plant actin filaments in vivo and visualizes the actin cytoskeleton in growing pollen tubes. Plant J. 16, 393–401.

Kost, B., Spielhofer, P., Mathur, J., Dong, C.-H., Chua, N.-H., 2000. Non-invasive F-actin visualization in living plant cells using a GFP-mouse talin fusion protein. In: Staiger, C.J., Baluška, F., Volkmann, D., Barlow, P.W. (Eds.), Actin: A Dynamic Framework for Multiple Plant Cell Functions. Kluwer Academic Publishers, Dordrecht, The Netherlands, pp. 637–659.

Kovar, D.R., Staiger, C.J., Weaver, E.A., McCurdy, D.W., 2000. AtFim1 is an actin filament-crosslinking protein from Arabidopsis thaliana. Plant J. 24, 625–636.

Li, S., Blanchoin, L., Yang, Z., Lord, E.M., 2003. The putative *Arabidopsis* arp2/3 complex controls leaf cell morphogenesis. Plant Physiol. 132, 2034–2044.

Mathur, J., Spielhofer, P., Kost, B., Chua, N.-H., 1999. The actin cytoskeleton is required to elaborate and maintain spatial patterning during trichome cell morphogenesis in *Arabidopsis thaliana*. Development 126, 5559–5568.

Mathur, J., Mathur, N., Hülskamp, M., 2002. Simultaneous visualization of peroxisomes and cytoskeletal elements reveals actin and not microtubule-based peroxisome motility in plants. Plant Physiol. 128, 1031–1045.

Mathur, J., Mathur, N., Kirik, V., Kernebeck, B., Srinivas, B.P., Hülskamp, M., 2003a. *Arabidopsis* CROOKED encodes for the smallest subunit of the ARP2/3 complex and controls cell shape by region specific fine F-actin formation. Development 130, 3137–3146.

Mathur, J., Mathur, N., Kernebeck, B., Hülskamp, M., 2003b. Mutations in actin-related proteins 2 and 3 affect cell shape development in *Arabidopsis*. Plant Cell 15, 1632–1645.

McCurdy, D.W., Kim, M., 1998. Molecular cloning of a novel fimbrin-like cDNA from *Arabidopsis thaliana*. Plant Mol. Biol. 36, 23–31.

Muday, G.K., 2000. Maintenance of asymmetric cellular localization of an auxin transport protein through interaction with the actin cytoskeleton. J. Plant Growth Regul. 19, 385–396.

Muday, G.K., Hu, S., Brady, S.R., 2000. The actin cytoskeleton may control the polar distribution of an auxin transport protein. Gravit. Space Biol. Bull. 13, 75–83.

Nishimura, T., Yokota, E., Wada, T., Shimmen, T., Okada, K., 2003. An *Arabidopsis* ACT2 dominant-negative mutation, which disturbs F-actin polymerization, reveals its distinctive function in root development. Plant Cell Physiol. 44, 1131–1140.

Ramachandran, R., Christensen, H.E.M., Ishimaru, Y., Dong, C.-H., Chao-Ming, W., Cleary, A.L., Chua, N.-H., 2000. Profilin plays a role in cell elongation, cell shape maintenance, and flowering in *Arabidopsis*. Plant Physiol. 124, 1637–1647.

Reichel, C., Mathur, J., Eckes, P., Langenkemper, K., Koncz, C., Schell, J., Reiss, B., Maas, C., 1996. Enhanced green fluorescence by the expression of an *Aequorea victoria* green fluorescent protein mutant in mono- and dicotyledonous plant cells. Proc. Natl. Acad. Sci. USA 93, 5888–5893.

Ringli, C., Baumberger, N., Diet, A., Frey, B., Keller, B., 2002. ACTIN2 is essential for bulge site selection and tip growth during root hair development of *Arabidopsis*. Plant Physiol. 129, 1464–1472.

Šamaj, J., Ovecka, M., Hlavacka, A., Lecourieux, F., Meskiene, I., Lichtscheidl, I., Lenart, P., Salaj, J., Volkmann, D., Bogre, L., Baluška, F., Hirt, H., 2002. Involvement of the mitogen-activated protein kinase SIMK in regulation of root hair tip growth. EMBO J. 21, 3296–3306.

Šamaj, J., Baluška, F., Hirt, H., 2004. From signal to cell polarity: mitogen-activated protein kinases as sensors and effectors of cytoskeleton dynamicity. J. Exp. Bot. 55, 189–198.

Sawitzky, H., Liebe, S., Willingale-Theune, J., Menzel, D., 1999. The anti-proliferative agent jasplakinolide rearranges the actin cytoskeleton of plant cells. Eur. J. Cell Biol. 78, 424–433.

Sheahan, M.B., Rose, R.J., McCurdy, D.W., 2004. Organelle inheritance in plant cell division: the actin cytoskeleton is required for unbiased inheritance of chloroplasts, mitochondria and endoplasmic reticulum in dividing protoplasts. Plant J. 37, 379–390.

Sun, H., Basu, S., Brady, S.R., Luciano, R.L., Muday, G.K., 2004. Interactions between auxin transport and the actin cytoskeleton in developmental polarity of *Fucus distichus* embryos in response to light and gravity. Plant Physiol. 135, 266–278.

Timmers, A.C., Niebel, A., Balague, C., Dagkesamanskaya, A., 2002. Differential localisation of GFP fusions to cytoskeleton-binding proteins in animal, plant, and yeast cells. Protoplasma 220, 69–78.

Voigt, B., Timmers, A., Šamaj, J., Hlavacka, A., Ueda, T., Preuss, M., Nielsen, E., Mathur, J., Emans, N., Stenmark, H., Nakano, A., Baluška, F., Menzel, D., 2005. Actin-based motility of endosomes is linked to the polar tip growth of root hairs. Eur. J. Cell Biol. 84, 609–621.

Volkmann, D., Baluška, F., 1999. Actin cytoskeleton in plants: from transport networks to signaling networks. Microsc. Res. Tech. 47, 135–154.

Wang, Y.-S., Motes, C.M., Mohamalawari, D.R., Blancaflor, E.B., 2004. Green fluorescent protein fusions to *Arabidopsis* fimbrin 1 for spatio-temporal imaging of F-actin dynamics in roots. Cell Motil. Cytoskeleton 59, 79–93.

Willemsen, V., Friml, J., Grebe, M., Van Den Toorn, A., Palme, K., Scheres, B., 2003. Cell polarity and PIN protein positioning in *Arabidopsis* require sterol methyltransferase1 function. Plant Cell 15, 612–625.

Xiang, C., Han, P., Lutziger, I., Wang, K., Oliver, D.J., 1999. A mini binary vector series for plant transformation. Plant Mol. Biol. 40, 711–717.